HIGH Tc SUPERCONDUCTORS FABRICATED BY PLASMA AEROSOL MIST DEPOSITION TECHNIQUE

X. W. Wang, K. D. Vuong, A. Leone, C. Q. Shen, J. Williams, and M. Coy
Alfred University, Alfred NY

ABSTRACT

We report new results on high T_c superconductors fabricated by a plasma aerosol mist deposition technique, in atmospheric environment. Materials fabricated are YBaCuO, BiPbSrCaCuO, BaCaCuO precursor films for TlBaCaCuO, and other buffers such as YSZ. Depending on processing conditions, sizes of crystallites and/or particles are between dozens of nano-meters and several micrometers. Superconductive properties and other material characteristics can also be tailored.

I. INTRODUCTION

Since the discoveries of high T_c superconductors between 1986 and 1993, different film fabrication techniques have been developed [1-3]. These techniques can be classified as thin film and thick film processes. The thin film processes include electron-beam evaporation, sputtering, and laser ablation [2,4-5]. The thick film processes include ink printing, tape casting, and plasma powder spray [6-8]. In the thin film processes, materials deposited onto the substrates can have atomic, ionic, or molecular sizes. Resulting thin films usually have high qualities and high densities. However, film growth rates in thin film processes are relatively slow, which could not be applied in large scale productions. As far as thick film processes are concerned, materials' sizes are 1-10 micrometers, film growth rates are relatively fast, but resulting films are usually inhomogeneous and porous. To find compromises between thin and thick film processes, other fabrication techniques have been developed such as pyrolysis chemical vapor deposition, mist deposition in microwave chambers [9], RF plasma mist deposition in enclosed chambers [10], and RF plasma mist deposition in atmospheric environment [11]. In this paper, we shall report new results obtained via the last process. Operational principles are briefly explained in section II, materials deposited are presented in section III, plasma-experimental conditions are given in section IV, results are summarized in section V, and future work is discussed in section VI.

II. OPERATIONAL PRINCIPLE

In this RF plasma aerosol deposition process, an aerosol mist containing desired cations is injected into a plasma region where the maximum temperature is 10,000 K and the gas pressure is slightly higher than one atmosphere. After vaporization and collision, ions or groups of ions with sufficient momenta travel towards a collector outside the plasma region. Depending on temperature profiles of the collector, nano-sized particles, particle clusters, or micro-sized deposits can be formed. In Figure 1, an experimental set up is illustrated, where the collector is a substrate with its heater block. Besides the substrate assembly, there are two other assemblies: starting material assembly and plasma

reactor assembly. The starting material assembly consists of an ultrasonic nebulizer, a solution container, a carrier gas inlet, and a mist outlet. The plasma reactor assembly consists of an RF coil with two copper leads (power supplied by an RF generator, 4 MHz, 35 kW), a plasma gas nozzle device with three plasma gas inlets, a quartz tube, a mist inlet, and a flame outlet. To prepare a solution, nitrates and/or chlorides with desired cations are dissolved in distilled water. The aqueous solution is poured into the solution container. When the ultrasonic nebulizer vibrates at a frequency of 1.63 MHz, the solution is excited into aerosol mist with droplet sizes of 5 - 10 micrometers. Under the pressure of a carrier gas (Ar), the mist is fed into the plasma reactor. After vaporization and deposition, films and/or materials are formed on the substrate (collector).

Around the middle section of the quartz tube, ion sizes are estimated to be 1 - 3 angstroms. Near the exit end of the tube (flame outlet), sizes of travelling particles are estimated to be 5 - 10 nanometers [12]. Particle clustering is expected to take place in the flame region, and nucleation is expected on the substrate. Besides substrate temperature, film morphology and grain sizes may be affected by the distance between the substrate and the flame outlet, plasma power coupled to the RF coil, plasma gas feeding rates, misting rates, and solution concentration. Oxidation process may be initiated in the quartz tube, enhanced by auxiliary oxygen supply near the flame outlet (not shown), and near the substrate.

III. MATERIALS DEPOSITED

A. BiSrCaCuO systems

In an earlier experiment, films with 2212 composition were fabricated with the plasma technique [13]. Recently, a group at SUNY Buffalo found that the 2223 fabrication window was approximately 5°C [10]. To ease fabrication conditions for large scale productions of 2223 film coatings, a bulk processing technique called two-powder process provided an alternate route [14]. In this bulk process, 2212 was first formed, 0011 was then added to form 2223.

In this work, we attemp to fabricate $Bi_{2.2-x}Pb_xSr_{2-y}Ca_{1+y}Cu_2O_8$ (2212) films; with x=0.20, 0.25, 0.30; and y = 0.25, 0.50, 0.75; as illustrated in Table I. Once 2212 film is formed, 0011 can then be added.

B. YBaCuO systems

Films of superconductive 123 phase were deposited at a substrate temperature of approximately 600°C, without post-annealing [11]. For a film deposited on MgO single crystal, superconductive transition temperature was 100 K, zero resistance temperature was 93 K, with transition width (10-90%) of 3 K [15]. It was observed that sizes of deposited oxides could be as small as 20 nanometers [16].

In this work, we attempt to fabricate nano-sized 211 powder. It is known that 211 affects the superconductivity of 123 phase. For example, the critical current (J_c) of 123 superconductor can be altered by the presence of 211 phase [17-18]. When J_c is enhanced, 211 particles are assumed to be flux pinning centers. When J_c is reduced, 211 particles are

assumed to be a micro-sized impurities blocking supercurrent flow. To clearly understand the roles played by the 211 phase, nano-sized particles are needed. Once these particles are produced with uniform particle size distributions, we can carry out well controlled doping experiments to systematically study pinning effects, kinetics, and mechanical properties.

C. BaCaCuO precursor films for TlBaCaCuO systems

In an earlier experiment, 0223 precursor films were deposited by the plasma technique. The precursor films were annealed at different substrate temperatures in a one-zone furnace to form 2212 and 2223 phases [19]. Recently, it was observed that 1223 phase has better critical current properties under high magnetic field than that of 2212 and 2223 phases. To fabricate a 1223 film, DeLuca developed a two-zone furnace technique [20].

In this work, we attempt to fabricate 0223 precursor films with different porosities and different dopants. When the porosity of a film can be tailored, we shall be able to control Tl diffusion processes in a two-zone furnace. When a metallic oxide such as silver oxide can be doped, we shall be able to align 1223 grains to enhance J_c.

D. Other buffer or hybrid materials

It has been a great challenge to coat YBaCuO on nickel containing substrates. If a buffer layer can be inserted between the substrate material and the superconductive material, this buffer layer can stop interdiffusion, can match lattice parameters, and can match thermal expansion coefficients. In this work, we attempt to deposit yttria stabilized zirconia, tin oxide, and silicon oxide. With superconductors, the last two coating layers can also be utilized as optical couplers and other hybrid optoelectronic films.

IV. PLASMA EXPERIMENTAL CONDITIONS

During plasma experiments, all parameters were optimized, as listed in Table II. In BiPbSrCaCuO experiments, nine batches of solutions were prepared according to the stoichiometric ratios listed in Table I. Each batch of films was deposited at two different substrate temperatures ranges. The low temperature range was from 400-600°C, while the high temperature range was 600-750°C. The films deposited at low substrate temperatures were heat treated in a furnace at 800°C for one hour to enhance 2212 phase formation. For comparative purposes, bulk powders were used to fabricate the superconducting phases represented by equations 1-9 [21]. These samples were prepared by a solid state reaction method. That is, powders of $CaCO_3$, CuO, $SrCO_3$, Bi_2O_3, and PbO were mixed in the ratios listed in Table I. These mixtures were then calcined and annealed in an atmospherically controlled furnace several times to form 2212 phases.

To prepare solutions for Y_2BaCuO_5, the stoichiometric ratios of Y:Ba:Cu ranged from (0.161) : (0.158) : (0.158) to (0.194) : (0.171) : (0.172). During fabrication of 211 materials, the collector (substrate) temperature was maintained at a temperature of 400 to 660°C.

To prepare solutions for BaCaCuO (0223), the mole ratio of Ba:Ca:Cu was 0.16:0.13:0.18 mole, with additional 0.01-0.02 mole of Ag in some experiments. The substrate temperatures ranged from 500 to 750°C.

To prepare yttria stabilized zirconia, zirconyl nitrate and yttrium nitrate powders (10 mol% yttrium) were mixed in the appropriate ratio and dissolved in distilled water. The substrate temperatures ranged from 600-950°C.

To prepare solution for tin oxide, $SnCl_4 \cdot 5H_2O$, HCl, and distilled water were mixed to produce solution with a concentration of 100 g/l. To prepare silica solution, a starting suspension containing silicon oxide powder (7 nm) and water was mixed to produce solution with a concentrations of 10 to 40 g/l.

V. RESULTS AND DISCUSSION

All films and materials were characterized by x-ray diffraction (XRD), energy dispersive spectroscopy (EDS), and scanning electron microscopy (SEM). Resistances of some films were measured by a four-point lead method, as a function of temperature.

1. BiPbSrCaCuO Films

From EDS measurements, all cations (metals) were observed in the BiPbSrCaCuO films. From SEM analysis, film thickness, morphology, and microstructures were studied. Film thicknesses were between 3 and 12 micrometers. As-deposited films contained plate-like crystals, with crystal sizes of 1-5 micrometers. However, crystal shapes were dependent on the cation ratios. Referring to Table I, crystals of equations 2-4, and 7-8 had more edges, indicating a more dendrite growth.

As verified by XRD measurements, when films were deposited at low substrate temperatures (<600°C), 2201 phase was the dominant phase along with 2212 and other binary and ternary phases as minor phases. After post-annealing at 800°C for one hour, 2212 phase was enhanced. However, when films were deposited at high substrate temperatures (>600°C), 2212 phase was the dominant phase in each as-deposited film as illustrated in Table I and Figure 2 (corresponding to Eqn. 7) [22]. There was also an indication of preferred 00l orientation, which indicated a possibility of liquid phase growth from small deposits in the ranges of 50 to 150 nanometers as determined from the Full Width Half Maximum (FWHM) of an XRD pattern by a program called SHADOW.

In comparison, a series of bulk processing experiments were conducted with nine identical equations listed in Table I. It took several thermal cycles to fabricate 2212 bulk materials. However, with this plasma technique, 2212 materials were synthesized within one deposition process.

2. Y_2BaCuO_5 (211)

Y_2BaCuO_5 powders were scrapped off a flat MgO collector (5cm x 5cm). XRD measurements revealed that powders were phase pure 211 when the starting material ratios were from (0.190) : (0.158) : (0.158) to (0.194) : (0.158) : (0.157) for Y:Ba:Cu, as

illustrated in Figure 3. As the ratios were outside of the range, other non-211 phases were presented as minor phases, as illustrated in Table III. The crystallite size increased from 53 to 116 nm when collector temperature increased from 500°C to 660°C. Initial SEM analysis of as-deposited powders revealed that these powders were agglomerated. Powders were then dispersed in acetone (containing Darvan 821 deflocculant), and vibrated in an ultrasonic oscillator. Particle sizes of those powders were approximately 100-300 nm, as estimated by SEM measurements.

3. BaCaCuO Precursor (0223)

For a precursor film, XRD reveals that barium copper oxide and calcium copper oxide phases were present. With silver dopant, silver metal was present from XRD pattern. The crystallite sizes ranged from 70-150 nm (from SHADOW). EDS results verified the existence of all desired cations. For the film deposited at 450°C, the particle sizes were relatively uniform (0.5-1.5 micrometers) and the film was porous. The film deposited at 650°C had particle sizes ranged from 0.5 to 10 micrometers and the film was dense. After thallination in a two-zone furnace, XRD revealed that the films were 1223 phase pure, and four-point-probe measurements revealed that zero resistance temperature was 108 K [23].

4. YSZ

Thin films of YSZ were deposited on Ni containing substrates. All as-deposited films were yttria stabilized cubic zirconia as determined by XRD. The deposition rate was dependent on the feed flow rate, reactor-substrate distance, nebulizer setting, and solution concentration. The film thicknesses ranged from 5 to 30 micrometers depending on the duration of deposition and other experimental conditions as those listed in Table I. The density and morphology of the film were dependent on the substrate temperature and deposition rate. It was observed that films deposited below 900°C have "snowflakes" appearance with low density and poor adhesion. When the substrate temperature was higher than 900°C, the film density and adhesion strength were increased. Post heat treatment slightly enhanced the density and adhesive strength of these films. Surface morphologies of the as-deposited and post heat-treated films were different. In general, the post-annealed films were more crystallized than the as-deposited films.

6. Tin Oxide and Silica

In tin oxide films, XRD revealed that the predominant phase was SnO_2 (Cassiterite - JCPDS card # 41-1445). Mossbauer spectrometry determined that the tin was in its $^{+4}$ oxidation state. The crystallite size was determined to be ~25 nm via XRD SHADOW program. SEM analysis of the films showed a particle size ranged from 0.4 to 4 micrometers. In addition, silicon oxide films were deposited on SLS glass substrates. When the solution concentration increased from 10-20g/l to 40g/l, films changed from amorphous to crystalline structures as verified by XRD and SEM.

VI. DISCUSSION

Plasma aerosol deposition technique has potential for large scale coatings such as underground superconductor cables and magnetic shieldings. To fully develop the technique into a mature process, we are currently conducting the following experiments:

1. to add (BiSrCaCuO) 0011 into 2212 to form 2223;
2. to dope nano-sized 211 powder into 123 superconductor and to compare the results with that obtained from the micro-size powder;
3. to hybridize 123 with others magnetic materials;
4. to improve the 0223 precursor film's properties by changing the experimental parameters, and to study the roles played by silver.

Acknowledgment

We would like to thank Dr. R.L. Snyder, Dr. S. Dorris, Dr. K. Gorreta, Mr. Robert Kampwirth, Mr. T. Hardy, Dr. C. Oberly, Dr. R.M. Spriggs, and Dr. L.D. Pye for their help. Part of the work was initiated at Argonne National Laboratory when Dr. X.W. Wang was a summer faculty of DOE Education Department. This work was partially supported by Argonne National Laboratory, U.S. Air Force, Center for Advanced Ceramic Technology, and NSF Industry Center for Glass Research.

REFERENCES

1. J. Talvacchio et al, "YBCO and LSCO Films Grown by Off-Axis Sputtering," in Science and Technology of Thin Film Superconductors 2, Ed. by R.D. McConnell and R. Noufi, Plenum Press, New York, 1990.
2. M. G. Krishna et al, "Single Source Electron Beam Evaporation of Bi-Sr-Ca-Cu-O Thin Films," in Science and Technology of Thin Film Superconductors 2, Ed. by R.D. McConnell and R. Noufi, Plenum Press, New York, 1990.
3. D. H. Kuo et al, "Preparation of Superconducting Tl-Ba-Ca-Cu-O Films by Diffusion Method," in Science and Technology of Thin Film Superconductors 2, Ed. by R.D. McConnell and R. Noufi, Plenum Press, New York, 1990.
4. N. G. Dhere et al, "Control of Thickness and Composition Uniformity in Sputtered Superconducting Thin Films," in Science and Technology of Thin Film Superconductors 2, Ed. by R.D. McConnell and R. Noufi, Plenum Press, New York, 1990.
5. T. Frey et al, "In-Situ Deposited Superconducting Laser Ablated Thin Films of $Y_1Ba_2Cu_3O_{7-x}$ and $Bi_{0.8}Pb_{0.2}Sr_{0.8}Ca_1Cu_{1.6}O_x$," in Science and Technology of Thin Film Superconductors 2, Ed. by R.D. McConnell and R. Noufi, Plenum Press, New York, 1990.
6. U. Balachandran et al, "Sintering $Bi_2Sr_2CaCu_2O_y$ Pellets and Thick Films," in Superconductivity and Ceramic Superconductors, Vol. 13, Ceramic Transaction, Ed. by K.M. Nair and E.A. Giess.

7. D. W. Johnson et al, "Processing and Jc Considerations in High-Temperature Superconductors," in Superconductivity and Ceramic Superconductors, Vol. 13, Ceramic Transaction, Ed. by K.M. Nair and E.A. Giess.
8. T. Okada, H. Hamatani, and T. Yoshida, "Radio-Frequency Plasma Spraying of Ceramics," J. Am. Ceram. Soc., 72 [11] 2111-16 (1989).
9. A. Koukitu et al, Jpn. J. of Appl. Phys. 28, L1212 (1989).
10. A. Shah, S. Patel, E. Narumi, and D. T. Shaw, "In situ, rf plasma deposition of $Bi_2Sr_2Ca_2Cu_3O_x$ thin films at atmospheric pressure," Appl. Phys. Lett. 62 (19) 2422-24, 1993.
11. X.W. Wang, H.H. Zhong, and R.L. Snyder, Appl. Phys. Lett. 57 (15) 1581 (1990).
12. T. Yoshida, "The Future of Thermal Plasma Processing," in Materials Transactions, JIM, Vol. 31, No. 1 (1990), pp. 1-11.
13. R.L. Snyder, X.W. Wang, and H.H. Zhong, U.S. Patent No. 5,120,703, June 1992.
14. Process developed by S. Dorris and B.C. Prorok at Argonne. For detailed information, see, for example, B.C. Prorok, "Formation of the $Bi_2Sr_2Ca_2Cu_3O_x$ Superconductor by a Two Powder Process," U. of Illinois at Chicago, 1993.
15. H.H. Zhong, X.W. Wang, J. Hao, and R.L. Snyder, "Deposition of Superconductive YBaCuO Films at Atmospheric Pressure by RF Plasma Aerosol Technique," in Superconductivity and Its Applications, Ed. by Y.H. Kao, A.I. Kaloyeros, and H.S. Kwok, AIP Conference Proceedings 251, Buffalo, NY 1991.
16. J. Hao, X. W. Wang, and R. L. Snyder, "RF Plasma Aerosol Deposition of Superconductive $Y_1Ba_2Cu_3O_{7-x}$ Films at Atmospheric Pressure," in Proceeding of the Fourth National Thermal Spray Conference, Pittsburg, PA, 4-10 May 1991.
17. Donglu Shi, S. Sengupta, and J.S. Luo, "Extremely fine precipitates and flux pinning in melt-processed YBa2Cu3Ox," Physica C213 (1993) 179-184.
18. S. Jin, T.H. Tiefel, and G.W. Kammlott, "Effect of Y_2BaCuO_5 inclusions on flux pinning in $YBa_2Cu_3O_{7-x}$," Appl. Phys. Lett. 59 (5), 1991.
19. H.M. Duan, B. Dlugosch, A.M. Hermann, X.W. Wang, J. Hao, and R.L. Snyder, "Superconducting TlBaCaCuO Thin Films From BaCaCuO Precursors," in Superconductivity and Its Applications, Ed. by Y.H. Kao, A.I. Kaloyeros, and H.S. Kwok, AIP Conference Proceedings 251, Buffalo, NY 1991.
20. J.A. DeLuca, P.L. Karas, J.E. Tkaczyk, P.J. Bednarczyk, M.F. Garbauskas, C.L. Briant, and D.B. Sorensen, Physica C 205, 21 (1993).
21. Unpublished results from X.W. Wang's experiments performed at Argonne National Lab between May and June 1993.
22. The crystallite size for 2212 film (eqn. 7) was ~128 nm as determined from SHADOW. Also the electrical resistance was measured by a four-point lead method. For as-deposited films, superconductive transition temperature was 100 K for Equation 5 and 90 K for Equation 2. The zero resistance temperature was 58 K and 60 K for Equation 5 and Equation 2, respectively.
23. Work performed by Mr. Robert Kampwirth at Argonne National Laboratory.

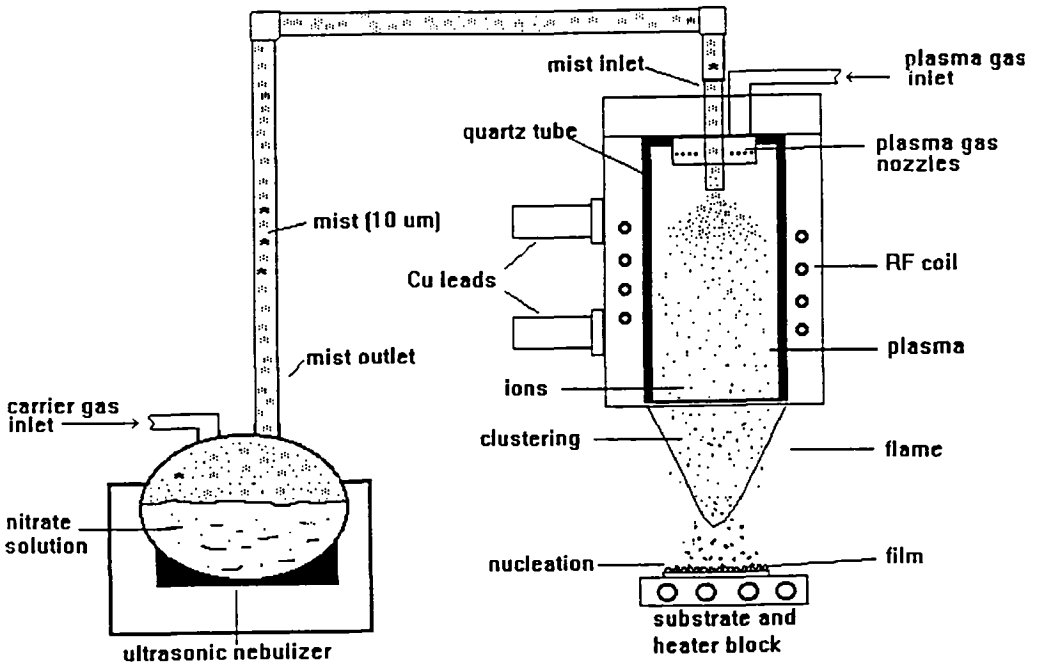

Figure 1. Plasma aerosol deposition experimental set-up.

Table I. Formulae of Nine Equations (Bi:Pb:Sr:Ca:Cu) and Relative Concentrations of 2212 Phases.

Equation #	x	y	Formula Ratio	2212*	2201	Ca_2CuO_3
1	0.20	0.25	2:0.20:1.75:1.25:2	89%	11%	0%
2	0.25	0.50	1.95:0.25:1.50:1.50:2	94%	4%	2%
3	0.30	0.75	1.90:0.30:1.25:1.75:2	93%	5%	2%
4	0.20	0.50	2:0.20:1.50:1.50:2	93%	6%	1%
5	0.25	0.75	1.95:0.25:1.25:1.75:2	86%	10%	1%+
6	0.30	0.25	1.90:0.30:1.75:1.25:2	95%	4%	1%
7	0.20	0.75	2:0.20:1.25:1.75:2	97%	2%	1%
8	0.25	0.25	1.95:0.25:1.75:1.25:2	95%	4%	1%
9	0.30	0.50	1.90:0.30:1.50:1.50:2	90%	8%	2%

* The relative percentages of various phases were estimated from relative heights of the 100% peaks.
+ other peaks observed

Table II. Film Deposition Conditions for Superconducting and Nonsuperconducting Materials.

Parameter	Bi-2212	Y_2BaCuO_5	$Ba_2Ca_2Cu_3O_x$	YSZ	SnO_2 / Silica
Power Setting %	35	35	30	30	40
Axial Argon Flow Rate (L/min)	5	7	7 - 9	7	5
Swirl Argon Flow Rate (L/min)	10	7 - 10	8 - 10	10	7.5
Swirl/Tangential O_2 Flow Rate (L/min)	15	10 - 15	15 - 20	10	12.5
Feed Argon Flow Rate (L/min)	4	2.5 - 4	3.5 - 5	2.5	2.5
Nebulizer Setting (%)	80	80	75	80	50 / 100
Substrate Distance (cm)	13	12	13	12	11
Substrate Temp. (°C)	400 - 750	400 - 660	500 - 750	600 - 950	400 - 500
Solution Conc. (g/l)	100	120	100	75 - 100	100 / 10-50

Table III. Solution Ratios and Substrate Temperatures Effect of Impurity and Crystallite Size.

Experimental #	Solution Mole Ratio (Y:Ba:Cu)	Substrate Temp (°C)	Impurity	Crystallite Size (nm)
1	0.190 : 0.158 : 0.158	660	0	105
2	0.190 : 0.158 : 0.158	500	10% Y2O3	116
3	0.190 : 0.158 : 0.158	500	10% Y2O3	102
4	0.161 : 0.158 : 0.158	400	30% 123	66
5	0.190 : 0.171 : 0.172	530	15% 123	56
6	0.190 : 0.164 : 0.163	600	15% 123	80
7	0.190 : 0.159 : 0.157	550	10% 123	72
8	0.194 : 0.158 : 0.157	570	0	70
9	0.192 : 0.158 : 0.157	500	0	53

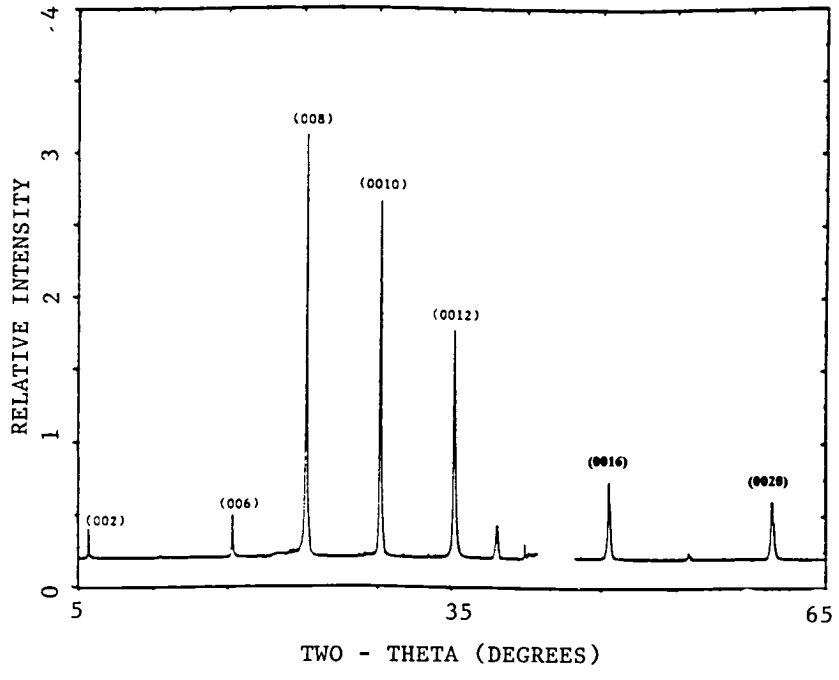

Figure 2. XRD pattern of 2212 film (eqn. 7). The peak at ~38 degree two-theta is due to MgO substrate. The peaks (omitted) between 42 and 45 degrees two-theta are also due to MgO substrate.

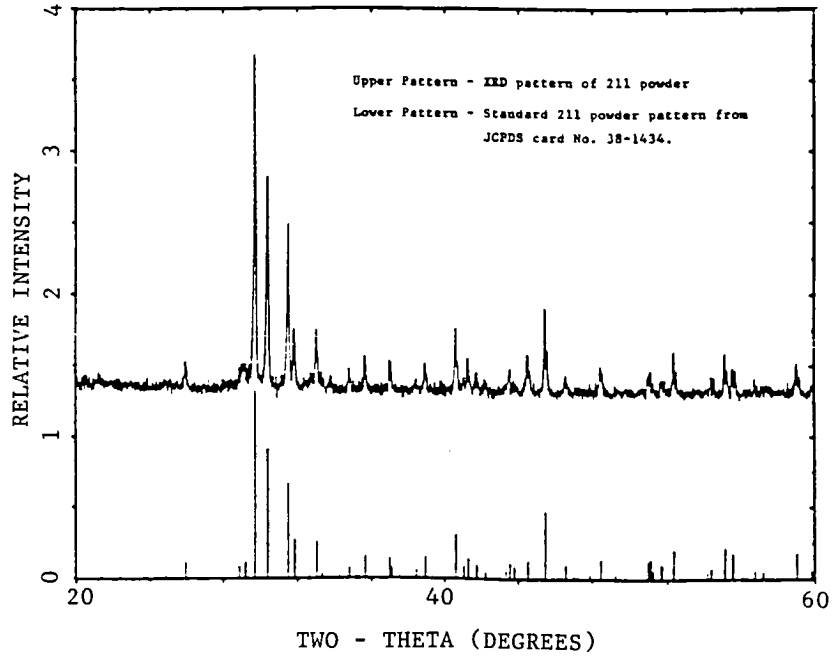

Figure 3. XRD pattern showing phase pure 211 powder (expt. #1).